2005 HST Calibration Workshop
Space Telescope Science Institute, 2005
A. Koekemoer, P. Goudfrooij, and L. Dressel, eds.

STIS Calibration Enhancement

P. Bristow, F. Kerber and M. Rosa

Space Telescope European Co-ordinating Facility, ESO, Karl-Schwarzschildstr 2, 85748, München, Germany

Abstract. The Instrument Physical Modelling Group in the Space Telescope European Co-ordinating Facility has undertaken to examine aspects of STIS calibration and develop physical model based solutions where appropriate. Here we discuss two such aspects and the status of the model based solutions. The first concerns the derivation of dispersion solutions for the echelle spectroscopy modes. The second corrects two dimensional CCD data (imaging and spectroscopic) for the effect of imperfect charge transfer in the read out process.

1. Introduction

The STECF Calibration Enhancement effort for the Space Telescope Imaging Spectrograph (STIS-CE) aims to improve data calibration via the application of physical modelling techniques. A high quality data reduction pipeline for STIS, known as CALSTIS, has been developed by, and is maintained by, the Space Telescope Science Institute (STScI) and the instrument definition team at Goddard Space Flight Centre (GSFC), see for example Dressel and Davies (2004) and Proffitt et al (2002) and references therein. This provides users with a rigourous, thorough and reliable calibration based largely on empirical techniques.

On the other hand, STIS-CE concentrates on some aspects of the pipeline where physical modelling may offer some improvement over empirical fits. The performance of existing components of the pipeline provide the obvious benchmark for the success of alternative techniques which we have developed. Hence, in what follows we will often make comparisons between the results of STIS-CE and those of CALSTIS. Whilst we are able to claim some significant improvements, it is testimony to the quality of CALSTIS that it has been quite a challenge to achieve these improvements even for the tasks which we considered most suited to a modelling approach.

Here we focus on two quite different calibration tasks: deriving the dispersion relation for echelle modes and correcting for charge transfer effects in the CCD readout. In both cases we begin by discussing the existing empirical approach. We do this for several reasons. Firstly this helps to introduce the calibration task we are trying to perform and provides a context for our description of the modelling approach. Secondly a description of the empirical approach is helpful for the comparisons that we will make later. Finally, since we began STIS-CE after STIS was already in orbit and the calibration plan was already well established, we were constrained to develop an approach which would take advantage of existing calibration data.

2. Wavelength Calibration

2.1. Empirical Approach

The empirical approach employed in CALSTIS is described in some detail in McGrath et al (1999). The basic principle can be briefly summarised as follows:

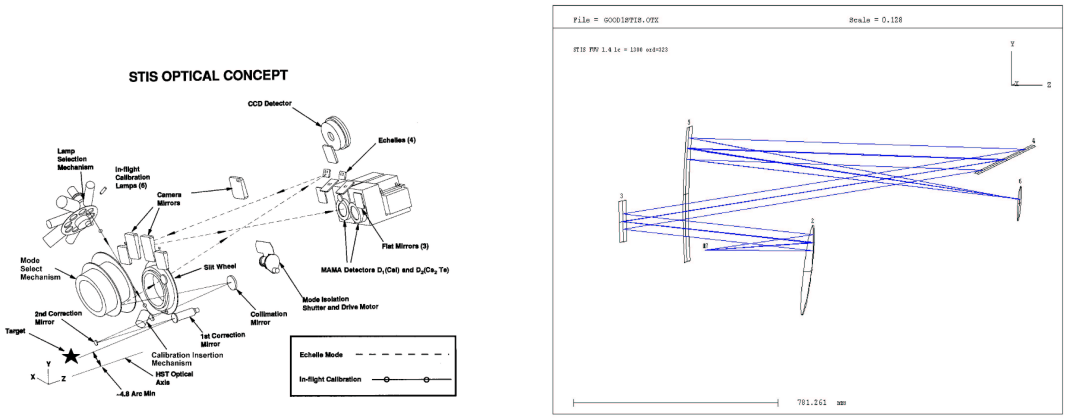

Figure 1.: The optical path of the STIS Echelle represented as a simple ray trace.

1. For each mode:
   - Dedicated deep calibration exposures of the onboard calibration lamps are obtained periodically.
   - Known features in the lamp or star features are identified and a polynomial fit is made which maps pixel positions in a given order to wavelength.
   - The result is stored as a master table for each mode.
2. For science exposures:
   - A short wavelength calibration, hereafter *wavecal*, exposure is made immediately before or after the science exposure.
   - The pipeline reduction determines the appropriate polynomial solution for the mode.
   - Cross correlation allows the determination of zeropoint offsets between the contemporaneous wavecal and the polynomial solution.

The essential ingredients here are the deep and short wavecal exposures and a reliable list of spectral features for the calibration lamp or standard star used. Kerber et al in this volume (2 refs?) describe a project which has improved our knowledge of the spectrum emitted by the Pt/Cr-Ne calibration lamps carried by STIS.

2.2. Simple Ray Trace Model

The design of modern astronomical instruments takes advantage of advanced optical modelling software, so we have a detailed knowledge of the optical path. However, this knowledge is not traditionally used in the calibration. In order to replace the polynomial dispersion with a physically motivated model, we used our knowledge of the optical components to build a simple ray trace of the STIS optical path, by representing optical surfaces as a series of matrix transformations. In this way were able to compute the eventual detector location of a ray of any wavelength. Of course this ray trace will only describe STIS if the various tips, tilts and other properties of the components are all accurately present in the matrices. Furthermore, some of these parameters will be mode dependent and others may change in a less predictable way with time.

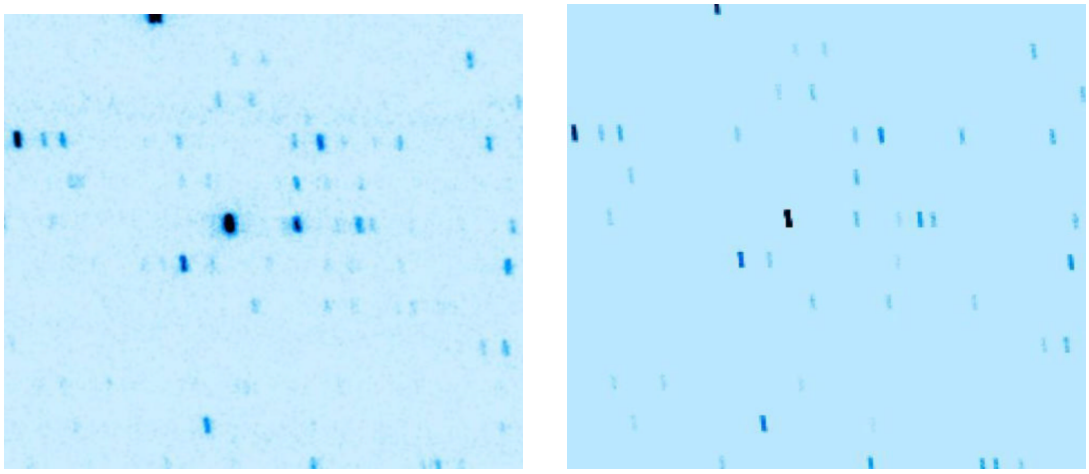

Figure 2.: On the left is a section of an exposure of the calibration lamp (E140H), whilst on the right is a simulation produced with the model and a spectral atlas for the lamp.

2.3. Optimisation

In order to obtain the precise values of these parameters we go first to the same deep wavecals as used by the empirical approach and require that the model accurately reproduces the distribution of spectral features in the detector plane. However, even our streamlined ray trace of STIS requires no less than 35 parameters. Clearly a trial and error approach is not feasible. Consequently we employ an optimisation process known as Simulated Annealing (SA) **??**. We provide the optimisation routine with a list of wavelengths of known features and their detector locations in the wavecal exposure. The SA algorithm then iteratively calls the optical model while adjusting the parameters and attempting to minimise the difference between the model predicted detector positions for these features and the values measured in the wavecal. The result of this process is a model parameter configuration file which accurately describes the state of the instrument at the time of the deep wavecal exposure.

2.4. Specialisation to Short Wavecals

Just as the empirical calibration requires an additional shift in order for the polynomial derived from deep wavecals to fit the contemporaneous short wavecal, the model based approach also makes use of fine tuning. By examining the differences between the optimised configurations obtained for a range of different wavelength settings we identified two parameters (both angles describing the orientation of the cross-disperser) as being critical. Therefore, when fine tuning to the configuration for a given observation a more physical approach than an x,y shift in the detector plane is to adjust these two parameters. This is achieved by applying SA once again, this time requiring that features in the short contemporaneous wavecal are matched and allowing only the two critical parameters to vary.

2.5. Visualisation Tools

Once we have determined the configuration of the model components in this way we can use the model to produce simulated data and other "visualisation products" with very little further effort. Figure 2 is an example using the calibration lamp line list. Given a model source spectrum and sky emission and absorption spectra, we could also simulate science data and use the model as an advanced exposure time calculator.

Another example is the creation of a map of the wavelengths across the detector generated with the model. In this map the pixel values are the wavelength of light that would

Figure 3.: Superpostion of a data frame and wavelength map. In practice the simplest way to use such a wavemap would be to blink between the data frame and wavemap in a FITS viewer such as DS9.

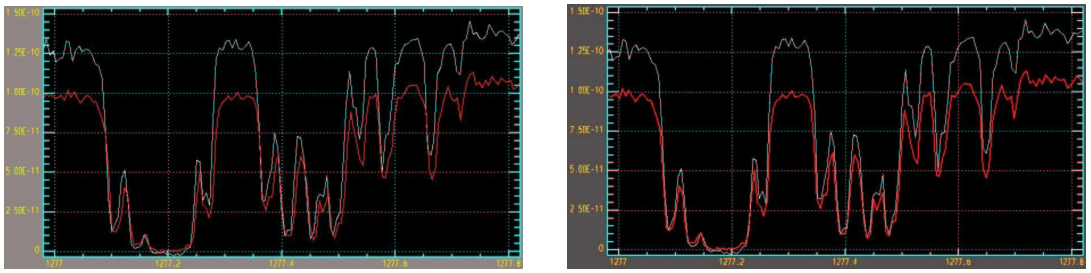

Figure 4.: Alignment between features in the overlap regions between two adjacent orders. The upper curve is order 329 and the lower is order 330. a) Empirical calibration. b) Model based calibration.

fall at this detector location. By loading both data and the corresponding wavemap into a FITS viewer such as DS9, pointing at a feature and blinking the images, the user gets a quick estimate of the wavelength of the feature, see figure 3.

2.6. Derivation of the Dispersion Relation

The visualisation tools described in the previous section are essentially just spin-offs of this approach. The real advantage is the more accurate dispersion relation that it offers. The ray trace itself is not reversible, so we cannot simply run it backwards to obtain the wavelength corresponding to the centre of each pixel. Instead we simply call the model for a list of wavelengths covering the range of the mode in question, these wavelengths are spaced finely enough such that the detector positions predicted are separated less than 0.5 pixel. Interpolation is then used to establish the wavelength corresponding to the centre of each pixel.

2.7. Science Case

As an example of scientific results which may be affected by this correction we identified a study of Thermal Pressures in the ISM by Jenkins & Tripp (2001). These authors actually noted inconsistencies in the *overlap regions* in their E140H data. The overlap regions are those parts of echelle spectral orders that contain wavelengths also present in previous or subsequent orders. Photons of the same wavelength may reach different locations on the

Figure 5.: Schematic diagram of the redistribution of charge that occurs during inefficient read out. a) An isolated point source. b) Two sources closely spaced in the readout direction.

detector, depending which order they are diffracted into. An accurate dispersion solution should assign the same wavelength to these photons (or rather the pixels they fall into) regardless of which order they are in. What Jenkins and Tripp noticed in their CALSTIS reduced data was a small shift between the wavelengths assigned to spectral features at one end of an order and those assigned to identical features at the beginning of the next (fig. 4a).

We used the model to compute a dispersion solution and found a much better fit (fig. 4b). Further analysis shows that typical offsets in order overlap regions in Jenkins and Tripp's data is of order 0.5 pixels. With the model this is typically reduced to 0.1 pixels. See Kerber et al (2006) in this volume for a more detailed discussion.

3. Charge Transfer Inefficiency (CTI)

By now, inefficient charge transfer is a well known source of photometry errors, degraded PSF and image artefacts (trails) in HST data. The magnitude of the effect increases with the amount of time a CCD detector is on orbit. Bombardment from energetic particles in the hostile radiation environment causes the build up of defects in the silicon lattice which trap charge during the transfer process. Hence WFPC2 data is the worst affected and even ACS data already shows measurable CTI. The removal of charge from large charge packets during readout clearly manifests itself as removal of flux from the central isophotes. Some of this charge is re-emitted in subsequent pixels and, in addition to the effects already mentioned, the centroid is shifted in the opposite direction to the readout.

Figures 5a and b show a grossly exagerated CTI effect, a) refers to an isolated point source and b) to two sources closely spaced in the readout direction. In both cases the solid curve represents the it true flux distribution and the dotted how it would appear after readout whit imperfect charge transfer. Also note that, the area under the dotted curve is, in reality, always less than that under the solid curve - not all charge is re-emitted. In figure 5b, the source nearer to the register looses charge in the same way as the isolated source in figure 5a. However, in doing so it fills the traps on the CCD in the pixels it is clocked through. As a result, when the charge packets from the second source are transferred through these pixels, many of the traps are already full. This results in less attenuation of charge from the second source. The tail following the second source is similar to that which followed the isolated source.These profiles could equally well represent the cross section (in the readout direction) of a stellar image, or the x-section of a spectrum.

3.1. Empirical Approach

The most dramatic impact upon scientific results is in the form of distorted photometric results from both imaging and spectroscopic data. This can be, to some extent, ameliorated by the use of an empirical formula which estimates the flux lost as a function of the

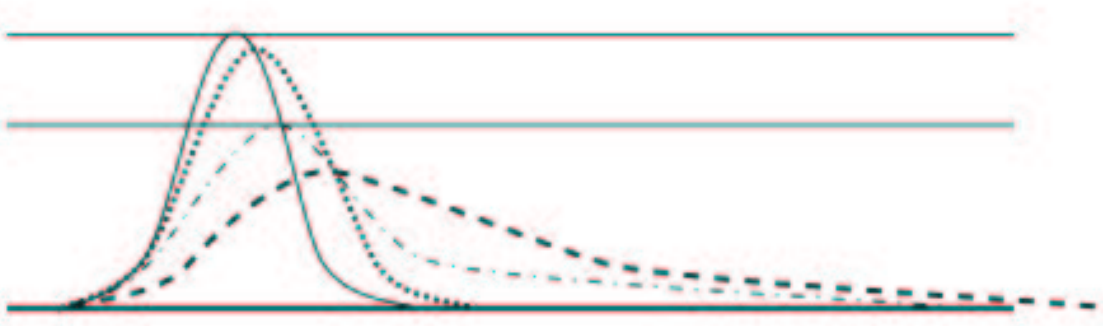

Figure 6.: Correction process (see text) illustrated for a point source. Once again, the CTI effects are grossly exaggerated for illustrative purposes

position on the chip, the flux of the source, the background level and the level of radiation damage (time on orbit). Goudfrooij & Kimble (2003) and Bohlin & Goudfrooij (2003) have calibrated such functions for STIS imaging and spectroscopic observations respectively.

However, this only applies to photometry, not astrometry (centroid shifts) or structure. Moreover, it only applies to the type of objects for which it was calibrated, to my knowledge this has only been attempted for point sources and must be separately calibrated for imaging and spectroscopic data and the calibration requires the acquisition of considerable calibration data. Finally this approach cannot account for the situation depicted in figure 5b, which makes it inappropriate in the case of crowded fields or extended objects.

3.2. Readout Model

A physical model based approach, in which CTI effects are understood in terms of the CCD operation and environment, has the potential to consider the flux distribution across the array, thereby returning flux to its true distribution. In addition to the photometry correction provided by the return of flux to central isophotes, the effects upon PSF and centroid and trails are also dealt with. Moreover such a correction applies equally to crowded fields and extended objects as well as point sources. In principle such an approach should be portable to other space based detectors.

We have developed a model (Bristow 2003a) which works in the following way: Starting from two arrays which describe the distribution of charge on a CCD after an exposure and the distribution of traps, we simulate the charge packet shifts that occur during readout keeping track of trapping, emission and dark current. Trap time-scales (as a function of operating temperature) are taken from laboratory data for three different defects known to occur in CCDs subjected to radiation damage. Also critical are the details of the chip architecture, in particular the clocking frequencies, well size and dark current.

3.3. Derivation of Correction

The readout model described is a "forward" model which cannot be run in reverse. So it is in fact only useful for adding CTI effects to data. That is, if we knew the "true" flux distribution (the solid line in figure 6), then the model would help us simulate the CTI degraded flux distribution (the dash-dot line). If we want to remove the effects then we need to proceed as follows:

- Since we have no other "best guess" with which to start the readout simulation, we use raw data from an exposure that is to be corrected.

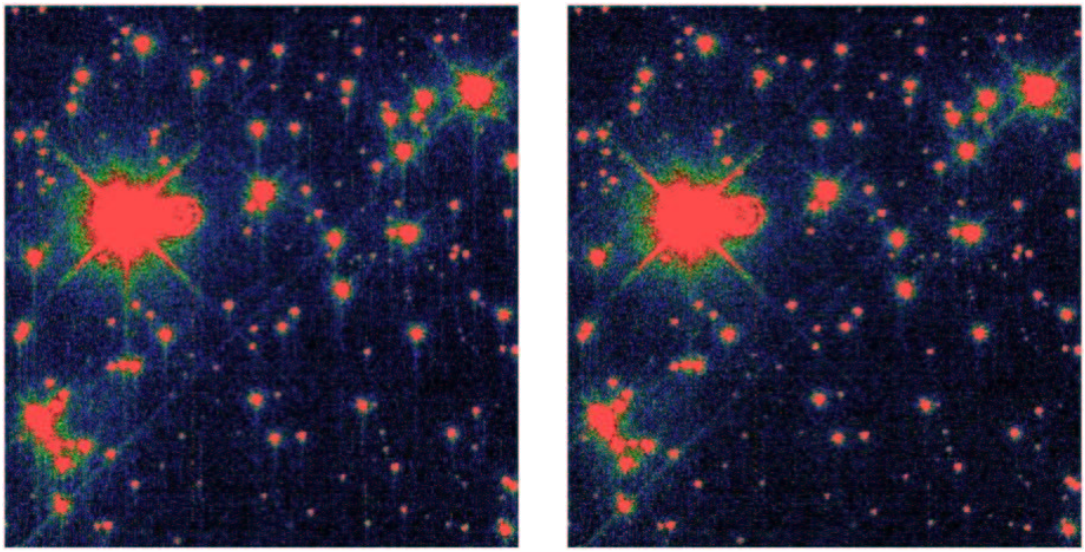

Figure 7.: Left: Raw STIS CCD imaging data. Right: The same data after correction with the readout model.

- The simulation then adds simulated CTI to this profile to give the dashed line.
- An improved estimate of the original profile can then be obtained by taking the difference between the dash-dot and dashed profiles and subtracting that from the red profile to get the dotted corrected profile. Essentially the difference between the dash-dot and dashed profiles represents the charge lost or gained due to CTI.
- Ideally we would run further iterations, taking the dotted corrected profile as input and so on. However, in practice, where the CTI effects are actually much smaller, one iteration is enough to restore 90-95% of the flux to the central isophotes.

This correction must be applied not only to all raw exposures in a dataset, but also to the associated dark and bias frames. This is discussed in detail in Bristow (2004a).

3.4. Validation

The removal of CTI trails can is illustrated in figures 7a and b, which show data before and after the application of the model based correction respectively.

In order to see how successfully the simulation derived corrections restore the photometric properties of CTI degraded sources we use the empirical corrections of Goudfrooij & Kimble (2003) as a comparison. These corrections have been calibrated for a range of epochs, background levels, source levels and distances from the readout register for a large number of datasets by using the ability of the STIS CCD to readout in two directions to registers at the top or bottom of the chip. As such they represent a distillation of the available data on CTI, so it is not necessary to repeat the exercies of extracting this information from the data.

Figure 8 represents such a comparison for a large sample of data and shows, on the whole, a good agreement between empirical and simulation derived corrections. There is however some scatter and a systematic overestimate from the simulation derived corrections relative to the empirical corrections as the corrections become larger (lower values in the plot). The scatter merely reflects the fact that the simulation deals with the actual, inherently noisy, charge distribution. Indeed the scatter represents the failing of the empirical solution for objects which are not bright point sources. If one considers only the bright

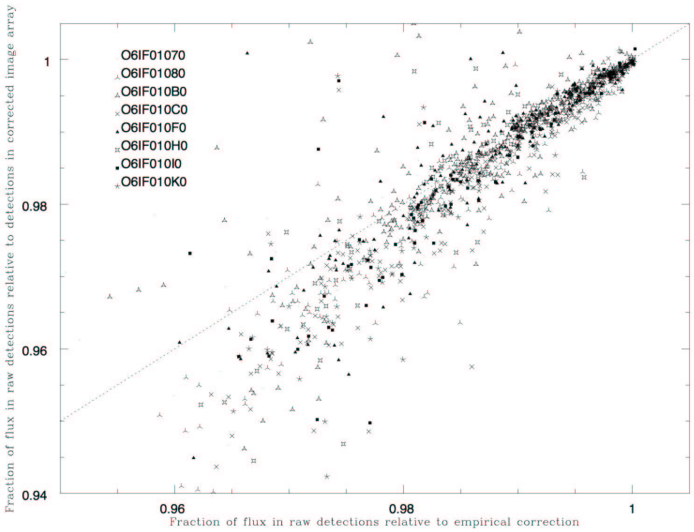

Figure 8.: Comparison between model and empirical photometric corrections for the flux within a 7 pixel diameter aperture. Detections come from the datasets according to the key in the figure. The dotted line represents perfect aggreement between model and empirical corrections.

point sources, as in figure 9, to which the empirical solution applies, then the agreement is much better. Examination of individual sources which fall far from the line of agreement in this plot almost always reveals some aspect (non-gaussian or faint profile or preceeding object nearby in the readout direction). These details are discussed in more detail in Bristow 2003b.

3.5. Science Case

The usefulness of this approach is best demonstrated by considering a science case for which astrometry is critical and where the existing empirical corrections have nothing to offer. The example we chose was a measurement of the proper motions of local dwarfs by making observations of constituent stars over a time base line of several years with STIS and WFPC2 (Piatek et al. 2002 & 2003). Each field was chosen to contain a background QSO as a truly stationary reference point. The analysis in the original AJ papers dealt with issues such as PSFs and geometric distortion in some detail. However the possible shift of the stellar centroids due to CTI was not considered.

To estimate the size of the effect we corrected the datasets used by Piatek et al for CTI and compared the new centroid position for all sources (figure 10). The crosses, fit by the solid line, are the CTI shifts in the earlier (April 2000) data. The squares, fit be the dotted line, are the CTI shifts in the later (April 2002) data. The CTI shift for the QSO at each epoch is ringed. As expected, a row dependent shift is apparent. If this were the same for each dataset and the QSO was close to the middle of the chip (which it is) then this would cancel out. However the gradient has steepened in the 2002 data due to the increased radiation damage. See Bristow (2004b) for further discussion.

The exact impact upon the final results, which utilise data from several fields at different inclinations for which the readout direction is different, is very hard to predict in this way so we provided Piatek et al with corrected data which they submitted to their detailed analysis. The effect upon the derived proper motions was found to be significant and appears to make the results from different fields more homogeneous and reduces the discrepancy between STIS and WFPC2 results (Presumably the outstanding disagreement with WFPC2 results

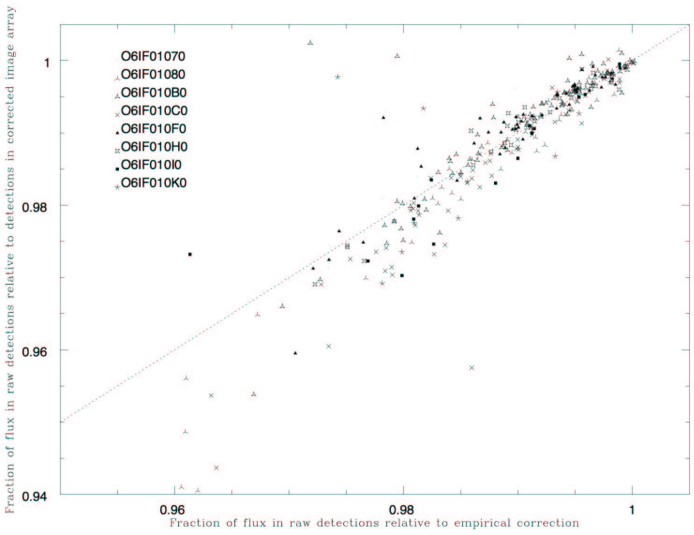

Figure 9.: As figure **??** except only showing sources for which the empirical correction is supposed to apply.

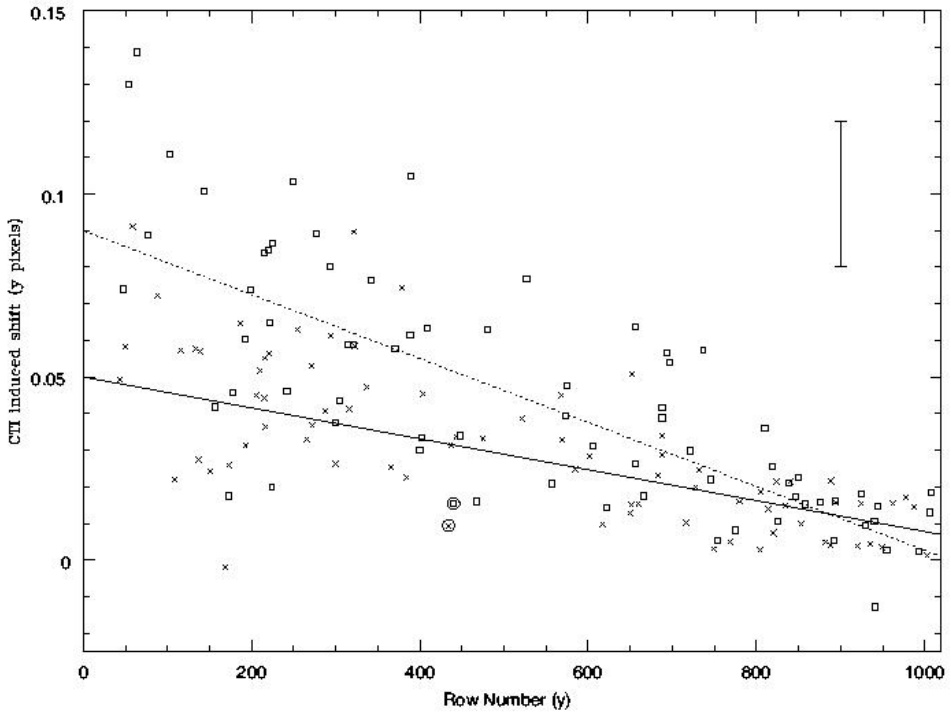

Figure 10.: CTI induced centroid y-shift for sources in the earlier epoch O5BL05010 (crosses) and later epoch O6D905040 (squares) datasets. The solid and dotted lines are linear fits to the O5BL05010 and O6D905040 data respectively. The QSO, as it appears in each image, is ringed. For comparison the error bar represents the scatter in centroid differences for sources from different epochs when put into the same reference frame in Piatek et al (2003).

is due to CTI in WFPC2 data), Piatek et al (2005). This has led to an ongoing collaboration with data for the dwarf galaxies Ursa Minor (published, Piatek et al 2005), Sculptor (in press) and Carina (processed).

4. Conclusions

We identified aspects of the STIS calibration procedure which lent themselves to a physical modelling approach and where we might expect such an approach to improve upon the already excellent performance of the CALSTIS pipeline. For two such aspects, STIS Echelle wavelength calibration and STIS CCD CTI correction, we developed the necessary physcial models and methods of application. These methods have been implemented, tested and applied to science cases yielding significant improvements with respect to the empirical approach.

References

Bohlin, R. and Goudfrooij, P., ISR 2003-03, 2003

Bristow, P., ST-ECF Newsletter pp9, No. 34, 2003a

Bristow, P., CE-STIS-ISR 2003-001, 2003b

Bristow, P., CE-STIS-ISR 2004-002, 2004a

Bristow, P., CE-STIS-ISR 2004-003, 2004b

Linda Dressel and James Davies, STScI Instrument Science Report STIS 2004-06, 2004.

Goudfrooij, P. & Kimble, R. A., 2003, in Proc. 2002 HST Calibration Workshop, ed. S. Arribas, A. Koekemoer, & B. Whitmore (Baltimore: STScI)

Jenkins, E.B. & Tripp, T.M., 2001, ApJS 137, pp297

Kerber et al. 2005 *These proceedings*

McGrath, M. A., Busko, I. & Hodge, P., STIS-ISR 99-03, 1999

Piatek, S., et al. 2002, AJ, 124, 3198

Piatek, S., et al. 2003, AJ, 126, 2346

Piatek, S., et al. 2005, AJ, 126, 2346

C. R. Proffitt, P. Goudfrooij, T. M. Brown, J. E. Davies, R. I.Diaz-Miller,L.Dressel,J.KimQuijano,J.Maz-Apellniz,B.Mobasher,M.Potter,K. C. Sahu, D. J. Stys, J. Valenti, N. R. Walborn, R. C. Bohlin, P. Barrett, I. Busko, and P. Hodge, 2003, in Proc. 2002 HST Calibration Workshop, ed. S. Arribas, A. Koekemoer, & B. Whitmore (Baltimore: STScI)